Ingeniare. Revista Chilena de Ingeniería
ISSN: 0718-3291
ingeniare@uta.cl
Universidad de Tarapacá
Chile

Echavarría, Aída M.; Bejarano G., Gilberto; Meza, J.M.
Mechanical and tribological features of TaN(Ag-Cu) duplex nanocomposite coatings: their response to heat treatment
Ingeniare. Revista Chilena de Ingeniería, vol. 25, núm. 4, diciembre, 2017, pp. 662-673
Universidad de Tarapacá
Arica, Chile

Mechanical and tribological features of TaN(Ag-Cu) duplex nanocomposite coatings: their response to heat treatment

Características mecánicas y tribológicas de recubrimientos nanocompuestos dúplex de TaN(Ag-Cu): su respuesta al tratamiento térmico

Aída M. Echavarría[1]* Gilberto Bejarano G.[1] J.M. Meza[2]

Recibido 26 de mayo de 2016, aceptado 3 de octubre de 2016
Received: May 26, 2016 Accepted: October 3, 2016

ABSTRACT

AISI 420 martensitic stainless steel samples and silicon (100) were coated with tantalum nitride doped with copper and silver nanoparticles TaN(Ag-Cu) to improve their hardness and wear resistance. The coatings were deposited by unbalanced DC Magnetron Sputtering technique, using a tantalum target and other silver/copper composite target (50/50%at), confronted each other. The coated samples were subjected to an appropriate heat treatment at 250 ºC for 8 minutes to achieve a controlled diffusion of Ag-Cu nanoparticles to the TaN(Ag-Cu) surface. Due to their mechanical and tribological properties depend, not only on the content of Ag-Cu, but also on the size, shape and density of nanoparticles of Ag-Cu on the surface of the coating. The influence of the Ag-Cu content on the microstructure and mechanical and tribological properties of the composite coating were evaluated before and after the heat treatment was evaluated. In general terms, the microhardness and wear rate increased initially with Ag-Cu content, but then dropped down for contents higher to 0.71% at, exhibiting the lubricating effect of Ag-Cu nanoparticles in the compound before and after heat treatment. The heat treated C3 sample showed a microhardness of 15 GPa, very superior to the hardness of AISI 420 stainless steel, as well as a wear rate six orders of magnitude lower than the steel.

Keywords: AISI 420, magnetron sputtering, silver and cooper nanoparticles, tantalum nitride, tribological properties.

RESUMEN

Se recubrieron muestras de acero inoxidable martensítico AISI 420 y de silicio (100) con nitruro de tantalio dopado con nanopartículas de plata y cobre TaN(Ag-Cu) para mejorar su dureza y resistencia al desgaste. Los recubrimientos fueron depositados por la técnica de la pulverización catódica DC asistida por campo magnético, utilizando un blanco de tantalio confrontado a otro blanco compuesto de plata/cobre (50/50 %at). Las muestras recubiertas se sometieron a un apropiado ciclo de tratamiento térmico a 250 ºC durante 8 minutos para lograr una difusión controlada de las nanopartículas Ag-Cu hacia la superficie del compuesto, ya que sus propiedades mecánicas y tribológicas dependen, no solo del contenido de Ag/Cu, sino también del tamaño, forma y densidad de las nanopartículas de Ag-Cu sobre la superficie del TaN (Ag,Cu). Se evaluó la influencia del contenido de Ag-Cu sobre la microestructura, las propiedades mecánicas y tribológicas del compuesto antes y después del tratamiento térmico

[1] Centro de Investigación, Innovación y Desarrollo de Materiales-CIDEMAT. Facultad de Ingeniería. Universidad de Antioquia. Calle 70 Nº 52-21. Medellín, Colombia. E-mail: aida.echavarria@udea.edu.co; gilberto.bejarano@udea.edu.co
[2] Tribology and Surfaces Group. Department of Materials and Minerals. Facultad de Minas. Universidad Nacional de Colombia. Calle 75 # 79A-51. Medellín, Colombia. E-mail: jmmezam@unal.edu.co
* Corresponding author.

En términos generales la microdureza y la tasa de desgaste aumentan inicialmente con el contenido de Ag/Cu, pero luego disminuyen para contenidos mayores a 0,71%at, exhibiendo el efecto lubricante que ejercen las nanopartículas de Ag-Cu en el compuesto. El recubrimiento C3 tratado térmicamente, presentó una microdureza de 15GPa, muy superior a la exhibida por acero inoxidable AISI 420, así como una tasa de desgaste seis órdenes de magnitud menor que la de dicho acero.

Palabras clave: AISI 420, pulverización catódica, nanopartículas de plata y cobre, nitruro de tantalio, propiedades tribológicas.

INTRODUCTION

AISI 420 stainless steel has widely being used in cutting tools manufacture and in the production of machine parts for the food, pharmaceutical and chemical industry, as well as in the design of surgical and dental devices, owing to its suitable corrosion resistance, good hardenability and high toughness [1-3]. Nevertheless, the average hardness obtainable in these types of steels of about 4.5 GPa is not high enough for some tribological applications, leading to premature wear and failure of parts when operating under severe working conditions or during sterilization processes.

A strategic alternative to improve AISI 420 stainless steel wear resistance is the use of ceramic coatings such as TiCN, TiAlN, CrN, ZrN, among others [4-9]. The aim of this research work was the improvement of the hardness and wear resistance of the AISI 420 stainless steel through a duplex surface treatment consisting of plasma nitriding of the steel, followed by the deposition of a TaN coating doped with Ag and Cu nanoparticles.

Given the properties of the individual elements of TaN(Ag-Cu) nanocomposite, TaN offers high hardness, good corrosion and wear resistance due to their covalent bonds, thermal and chemical stability [10-12]. Meanwhile soft silver and copper nanoparticles are immiscible in the TaN and incorporated into the ceramic matrix, generating a self-lubricating effect and improving the tribological properties [13-15].

Despite the positive effect of nanoparticles of silver and copper on the tribological properties, they also depend not only on their shape, size, density and distribution in the ceramic matrix [16-18] but also on the content of Ag and Cu in the compound and on an appropriate heat treatment cycle of the coated samples. These parameters were studied in this as well.

EXPERIMENTAL METHODS

TaN(Ag-Cu) coatings development

TaN(Ag-Cu) coatings were deposited on AISI 420 steel plates (12.5x12.5x2.8 mm^3) and single crystalline silicon wafers (100) by unbalanced DC magnetron sputtering, using a tantalum target and an Ag/Cu (50-50%at) composited target, both with 99.9% purity and dimensions of 500x100x6 mm^3. A rectangular vacuum chamber with dimensions of 500x500x800 mm^3 was used in this work.

Silicon substrates were used for spectroscopic and X- ray diffraction measurements to reduce the signal from the alloying elements of steel. AISI 420 stainless steel samples were polished using SiC emery paper with grain sizes between 300 to 1200 and subsequently polished to a mirror finish until obtaining an average roughness of Ra= 0.05μm in alumina aqueous solution. The polished samples were cleaned in an ultrasonic bath with an alcohol-acetone solution for 15 minutes and then subjected to argon ionic cleaning into the vaccum chamber during 30 minutes at a pressure of $1.7x10^{-1}$ mbar and using a bias voltage of –500V applied to substrates.

The nitriding process was performed into pulsed plasma conformed by Ar = 57 sccm, N_2 = 15 sccm and H_2 =27 sccm; the pressure, bias voltage and temperature of the process were fixed to 5.1x 10^{-1}mbar, –600 V and 380 ºC, respectively. This process was performed for 7 hours. The low temperature of plasma nitriding was used to avoid the precipitation of chromium carbides, conserving the corrosion resistance of steel 420.

Two subsequently Ta- and TaN- adhesion layers with a thickness of about 200 nm were deposited first on

the sample surface. The TaN (Ag-Cu) coatings were deposited during 3 hours and 40 minutes, keeping a constant power of 1500 W applied to Ta-target and varying the power supplied to Ag/Cu-target between 10 and 40W as is summarized in Table 1. The work pressure and temperature process were fixed in $5.2x10^{-3}$ mbar and 150 ºC, respectively. The low process temperature was chosen to avoid an uncontrolled growth of Ag-Cu nanoparticles. During deposition, the substrates were placed at 80mm in front to the targets, rotating at a constant speed of 20 r.p.m.

Coating characterization

Cross section and superficial microstructure and morphology of deposited coatings were examined by SEM in a JEOL 6490LV instrument equipped with EDX detector (error detector sensitivity 0.1%) to determine the elemental chemical composition of the coatings and the tribological tracks. One of the coatings, whose nanoparticles of Ag-Cu were not resolved with the SEM, was evaluated by Atomic Force Microscopy (AFM) by Multitarea Auto probe CP instrument in a resistive mode applying a current between the conductive tip and the coating surface and then amplifying the current signal of the conductive points where the Ag-Cu nanoparticles were located.

Phases composition were established with an X-ray diffractometer from the brand Panalytical Empyream, using Cu Kα1 radiation with λ=1.540598 Å, 45 kV, 40 mA, an incidence angle of 1º and a step of 0.05º per second. XRD patterns were analyzed with High Score Plus software using Profile Fitting Refinement to calculate the offsets of the peaks of the possible formed phases and the crystallite size.

The value of the surface roughness (Ra) was the average of five measurements and was determined by a contact profilometer from the brand Bruker Pektakxt, applying a contact force of 3 mg for 30 seconds over a distance of 1500 microns, according to the ISO 4287:1998 standards.

A Shimadzu HMV-G20 was used to determine the knoop hardness of coatings and substrates, applying a load of 25 grf. The hardness and standard deviation value for each sample were calculated as the average of ten measurements, according to the ASTM C1326:13 standards. Friction coefficient and wear rate were evaluated in triplicate through ball-on-disc apparatus at a temperature of (19 ±2) ºC and relative humidity of (48.5 ±2)%, using an alumina counterbody (6 mm in diameter). Applying a load of 1N during 600 seconds on the sample, which rotated at a speed of 70 rpm, according to the ASTM G99-95 standards. Subsequently, volume loss was determined by a contact profilometer, using a load of 3 mg over a distance of 1000 microns.

RESULTS AND DISCUSSION

Coating's morphology and chemical composition

Coatings chemical composition with different powers applied to Ag-Cu target was determined by EDX spectroscopy and is given in Table 1. The results indicated that the atomic percentage content of silver, copper and nitrogen gradually increases with power applied to target, while the content of tantalum decreases.

Figure 1 shows the cross-sectional SEM images of the coatings deposited onto 420 stainless steel, it can be seen an increasing of the coating thickness as the power applied to the Ag/Cu target is increased, which in turn increases the Ag-Cu content due to a higher sputtering rate of the Ag/Cu-target. All coatings have a uniform thickness (Figure 1), with a columnar structure for low contents of silver/copper (Figure 1a and 1b).

Table 1. TaN (Ag-Cu) coatings thickness and elemental chemical composition.

Coating	Ag/Cu Target power (W)	Thickness (µm)	Ag-Cu content (%at)	%at			
				N	Cu	Ag	Ta
C1	10	1.28	0.64	41.92	0.06	0.58	57.44
C2	20	1.88	0.71	42.90	0.09	0.62	56.38
C3	30	2.25	1.64	44.57	0.74	0.9	53.79
C4	40	3.18	2.87	45.82	1.22	1.65	51.31

However, such a structure almost disappears and is densified for contents of Ag/Cu greater than 0.71%, (Figures 1c and 1d). This behaviour is correlated with the fact that the Ag-Cu clusters have a high kinetic energy to achieve their rearrangement in the spaces between grain boundaries of the TaN matrix, conducting to a progressive densification of the coatings and thereby generating deformation of the crystal lattice of TaN. Similar results have been reported by Musil and Lloyd [19-20].

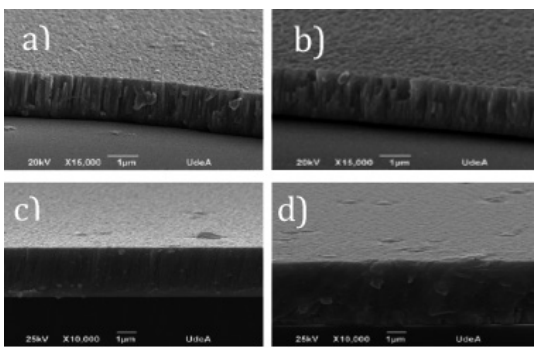

Figure 1. Cross section SEM micrographs of TaN(Ag-Cu) coatings. a) C1, b) C2, c) C3 y d) C4.

Structural analysis XRD patterns for the TaN(Ag-Cu) coatings and their chemical phases are shown in Figure 2. In all coatings, the face-centered-cubic phase (fcc) of TaN is observed, the preferential growth in the crystallographic direction (200) is observed for the lowest power of manufacture (10 W), its intensity decreases with increasing the amount of Ag-Cu (as the power is increased) and, the (111) and (220) directions are promoted.

In these patterns, isolated peaks of Ag appear, suggesting the insolubility of this element in the TaN-matrix without intermetallic compounds formation, as presented in the structural zone model (SMZ) by Barna and Adamik [21-22].

Ag phase starts to appear at a power of 20 watts, i.e. for C2 coating and its intensity rises with the power applied to the target. Just one Cu peak it is barely detected at the highest power, probably due to its low content [23, 24] and to the overlapping with the broad peak of the TaN (200) phase located. Located between 38.9º and 44.4º covering-up the copper peak

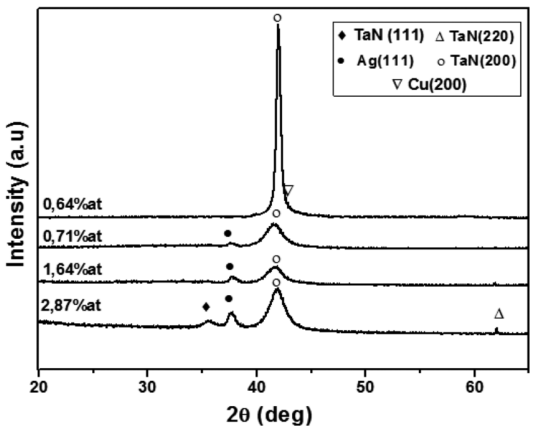

Figure 2. XRD patterns for TaN(Ag-Cu) coatings with different atomic percentages of Ag-Cu of the crystalline structure of TaN with increasing content of Ag-Cu.

of cubic phase in the direction (111), which normally diffracts in the 43.05 [º2Theta] position, according to the patron described in the ICSD 98-018-0109 index card. In this sense, the low Cu content in comparison with Ag is related with its lower sputtering rate, according to the chemical composition determined by EDX spectroscopy (Table 1). The inexistence of phases comprising Cu and TaN once again indicates the insolubility of Cu in the TaN matrix [25].

The diffraction angles for the main peaks of TaN and Ag of the manufactured coatings, as well as the crystallite size related to the content of Ag-Cu are reported in Table 2. The minimum rightward

Table 2. High Score Plus software with profile fitting refinement analysis of the XRD patterns TaN (Ag-Cu) coatings with different atomic percentages of Ag-Cu.

Phase	Ag-Cu content (%at)	Angle (2ºTh)	Crystallite size (Å)
TaN(200)	0.64	41.47	640.19
	0.71	41.61	257.17
	1.64	41.81	240.86
	2.87	41.98	144.20
Ag(111)	0.64	37.77	Not found
	0.71	37.75	136.03
	1.64	37.57	155.84
	2.87	37.33	553.07

shift observed at the peak of TaN (200) suggests the existence of residual tensile stresses in the coatings, caused by the increasing lattice deformation.

Heat treatments of TaN(Ag-Cu) coatings

Taking into account the positive effect of Ag-Cu nanoparticles on the friction coefficient and the wear resistance depends not only on the continued availability of the nanoparticles in the composite surface but also on its size, distribution and density [26]. Heat treatments of TaN (Ag-Cu) coatings were performed in a Nabertherm muffle furnace in a controlled nitrogen atmosphere.

Heat treatments at 250 ºC during 8 minutes were performed to induce the growth of Ag-Cu phase nanowire shaped and also to promote their diffusion to the coatings' surfaces through the columnar structure of TaN, as schematically illustrated in Figure 3. After the heat treatment, samples were cooled down with an air stream.

The diffusion temperature of 250 ºC was determined using scanning differential calorimetry (DSC) in Q200 instrument with a ramping rate, set at 100 ºC/s and a temperature range between 23º and 400 ºC, according to previous works by Tseng CC and coworkers [27]. For the heat treatment, these authors used a high cost oven for Rapid Thermal Annealing (RTA).

Figure 4 shows SEM micrographs of the surface of TaN(Ag-Cu) coatings in both conditions: as deposited

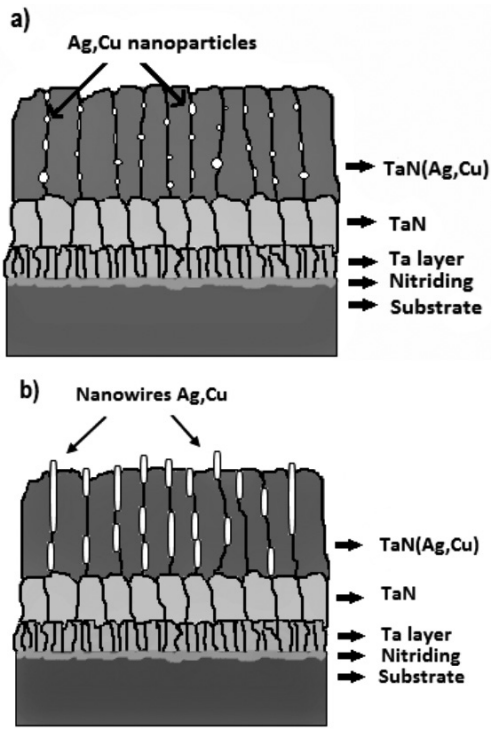

Figure 3. System configuration design TaN(Ag,Cu) coatings a) Ag-Cu nanoparticles before diffusion process and b) Ag-Cu nanowires formation on surface after heat treatment.

produced and after the heat treatment. Some Ag-Cu spherical nanoparticles and nanowires formed on coatings' surfaces after heat treatment are visible in

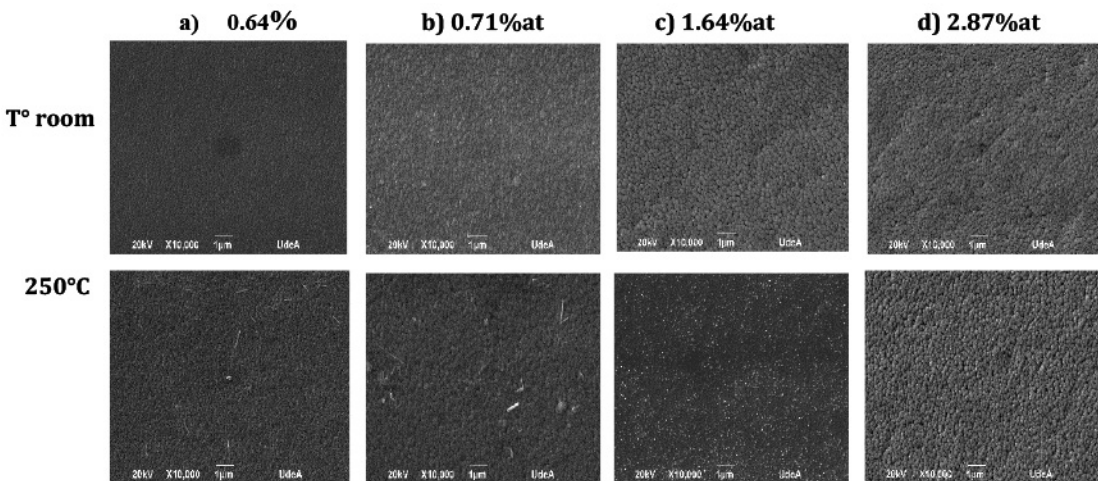

Figure 4. SEM micrographs of the surface of TaN(Ag-Cu) coatings in both conditions: as produced and after the heat treatment a) C1, b) C2, c) C3 y d) C4.

Figures 4a and 4b, while Figure 4c for de C3 coating shows quasi-spherical Ag-Cu nanoparticles with a higher density and a more homogeneous than the other coatings. Ag-Cu nanoparticles in C4 coating were not observed after heat treatment due to its small size, which was not resolved under the SEM (Figure 4d).

Therefore, this sample was analyzed by AFM using the resistive mode as shown in Figure 5, where Ag-Cu particles with an average diameter of 15 nm and located over the grain cupules of the TaN-matrix were observed. C3 coating was submitted to an additional heat treatment at 300 ºC, this was made to verify the temperature effect on the diffusion and growth of the nanoparticles and results are shown in Figure 6. In this case, the Ag-Cu nanoparticles formed on coating surface increased their size compared with the coating heat treated at 250 ºC;

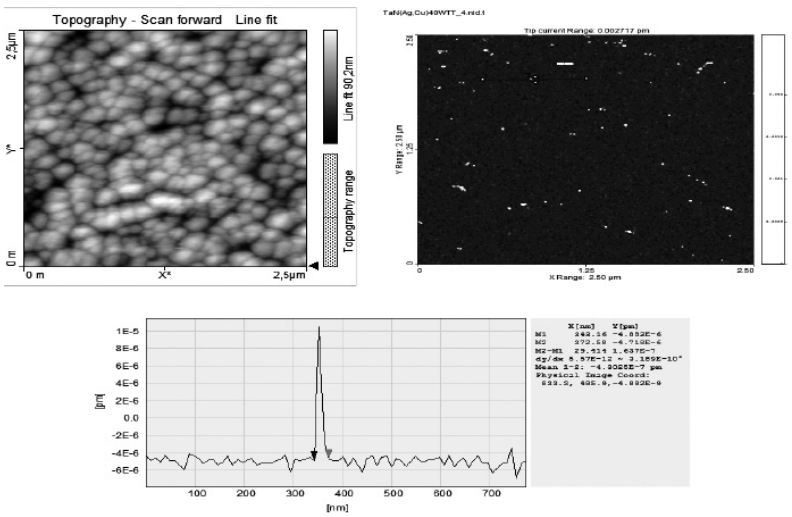

Figure 5. AFM images in resistive mode of the C4 coating after heat treatment at 250 ºC during 8 minutes.

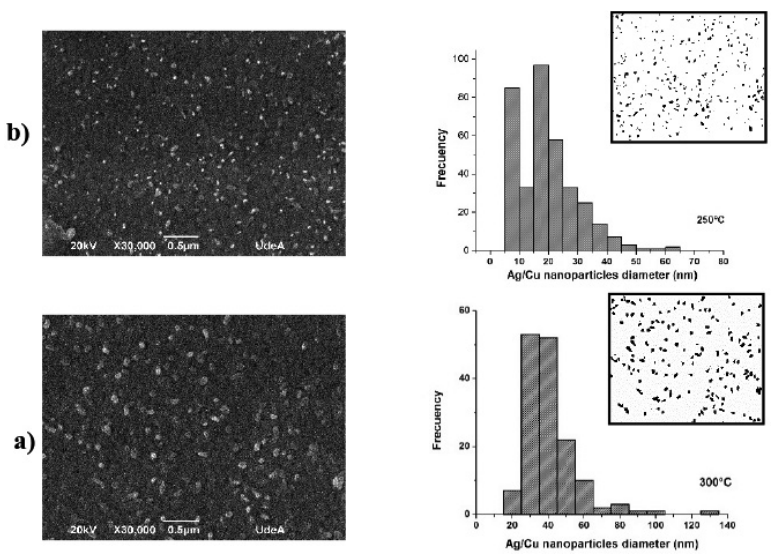

Figure 6. Surface SEM micrographs of C3 coating after heat treatment during 8 minutes and frequency vs. Ag-Cu nanoparticles diameter histograms a) 250 ºC and b) 300 ºC.

this event is related to the higher diffusion rate and greater coalescence process, which can lead to the formation of Ag-Cu clusters [28-30].

The binary images by Fiji ImageJ software were used to determine the diameter size range, results shown a higher frequency of small Ag-Cu nanoparticles for the C3 coating, treated at 250 ºC than the one treated at 300 ºC (Figure 6). At 250 ºC (Figure 6a), the coating showed nanoparticles with diameters less than 70 nm, and the highest frequency was found in the range of 15 and 20 nm, but there is a significant number of nanoparticles with diameters between 5 and 10 nm. Also, the diameter of nanoparticles in the coating treated at 300 ºC (Figure 6b) showed a maximum of 135 nm, but it exhibited the highest frequency in the range of 25 to 45 nm.

In this sense, the diameter of nanoparticles increases with temperature, as well as the frequency of bigger nanoparticles. The analysis above suggests that the average size of Ag-Cu nanoparticles of deposited coatings is statistically less than 100 nm and therefore the developed TaN(Ag-Cu) coating system can refer as a nanocomposite, being suited for biomedical [31-33] and nano-technological applications.

The elemental chemical composition of the heat-treated coatings are given in Table 3, compared with the coatings without heat treatment (Table 1), exhibited an enrichment of Ag-Cu on the surface due to the higher diffusion and growth of Ag-Cu nanoparticles during the heating process.

Average surface roughness (Ra) of deposited coatings before and after heat treatment is shown in Figure 7.

Table 3. Elemental chemical composition of TaN (Ag-Cu) coatings heat treated at 250 ºC during 8 minutes.

Coating	%at			
	N	Cu	Ag	Ta
C1	41.64	0.17	0.37	57.81
C2	40.04	0.10	0.92	58.94
C3	38.84	1.03	1.37	59.16
C4	40.68	4.04	2.00	53.27

It can be seen that the roughness of the coatings increases with the Ag-Cu content in both as deposited and heat treated conditions. Moreover, the heat-treating procedure increases the roughness regarding the deposited condition. This is probably associated with the fact that the more power of the manufacture the more the target yielding, which produces a change in the morphology of the layer, on the other hand the heat-treating increases the size of the nanoparticles and as they are present in the surface, the roughness is increased.

Microhardness and wear evaluation

As presented in Figure 8, Knoop hardness of the coated samples was between 13.5 and 20.6 Gpa, despite the influence of the substrate (because of the load used), this clearly is an improvement regarding the hardness of 420 steel (4.8 GPa) used as a substrate.

It was also found that microhardness initially increased with the increment of Ag-Cu, but then decreased for contents higher than 0.71%; this behaviour requires a detailed investigation to be explained. However, the crystalline orientation changes and the increasing amount of the silver phase as a function of the power of manufacture are possibly related to the changes in hardness. At high power the high soft silver phase content can explain the decreasing in hardness. Values of coefficient of friction and wear rate of deposited TaN(Ag-Cu) coatings.

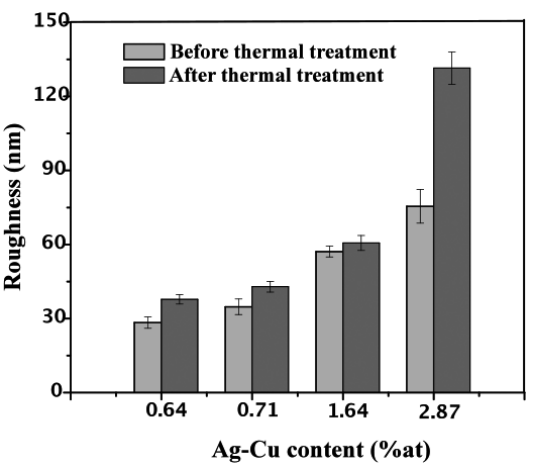

Figure 7. Average TaN(Ag-Cu) coatings roughness as function of Ag-Cu content before and after of heat treatment.

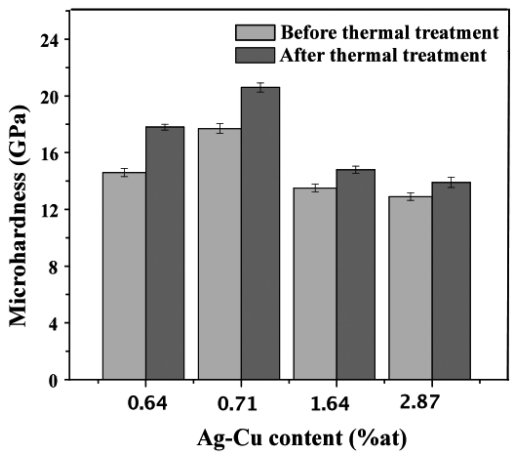

Figure 8. TaN(Ag-Cu) coatings Knoop microhardness as a function of their Ag-Cu content before and after of the heat treatment.

Values of coefficient of friction and wear rate of deposited TaN(Ag-Cu) coatings without and with heat-treatment are consigned in Table 4; the results of all tribological tests for the heat treated samples indicated a better anti-wear effect with increasing Ag-Cu content than the untreated ones. This improvement is linked to a surface enrichment of TaN with silver and copper nanoparticles, which have a solid lubricant effect that is more efficient than in untreated samples, as also explained by various authors [14,15], [34-36].

Figure 9 shows the wear tracks of C1 and C3 coatings, which after heat treatment are clearly smoother and shallower than as in the as produced condition (no heat treatment), decreasing removed material volume after tribological evaluation. In C1 coating, a mix of abrasive and adhesive wear was observed, generated by debris or hard particles detached from TaN and by the Ag-Cu nanoparticles deformed along the track and under pressure of the alumina counterbody (Figure 9a), explanation that is very consistent with the findings of Holmberg K. [37].

For C3 coating (Figure 9b), an adhesive wear mechanism can be observed, generated by the adhesion of the Ag-Cu particles to the alumina counterbody and by the deformation of the nanoparticles along the wear track, exhibiting the expected lubricating effect and an improvement of the tribological behaviour, particularly for the heat treated coatings, where a smooth and small wear track was observed.

Figure 10 shows the elemental chemical composition mappings of C1 without heat treatment and also for the heat treated C3 sample (Figure 10a).

The EDX test shows the presence of chromium and iron in some places, suggesting that the steel substrate was exposed because of abrasive wear of the coating.

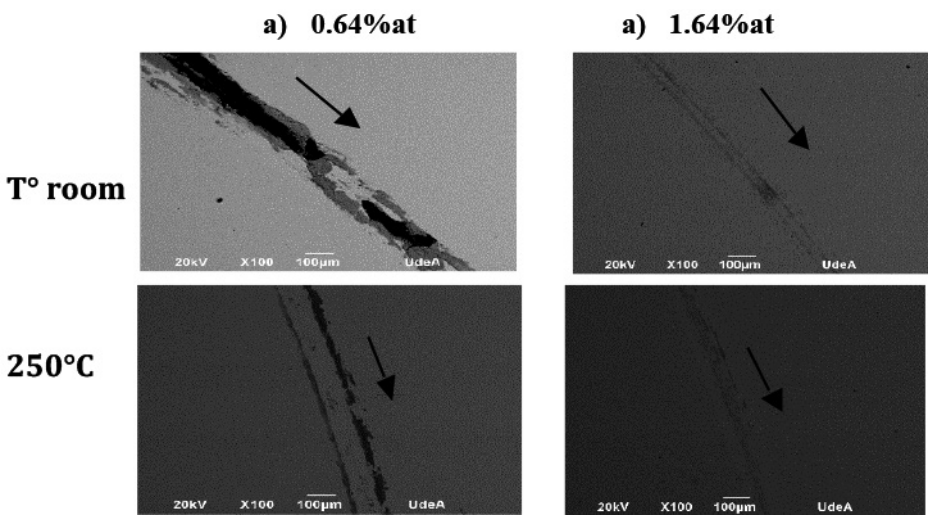

Figure 9. TaN(Ag-Cu) coatings wear tracks after and before heat treatments a) C1 and b) C3.

Table 4. TaN(Ag-Cu) coatings friction coefficient and wear rate values after and before of the heat treatments.

Coating	Friction coefficient before thermal treatment	Friction coefficient after thermal treatment	Wear rate before thermal treatment $m^3/(N.m)x10^{-15}$	Wear rate after thermal treatment $m^3/(N.m)x10^{-15}$
C1	0.42	0.22	30.7	9.14
C2	0.36	0.29	98.7	1.90
C3	0.46	0.19	132.3	1.50
C4	0.55	0.49	123.4	4.70
AISI 420 stainless steel	0.77	–	$2.0x10^{-9}$	–

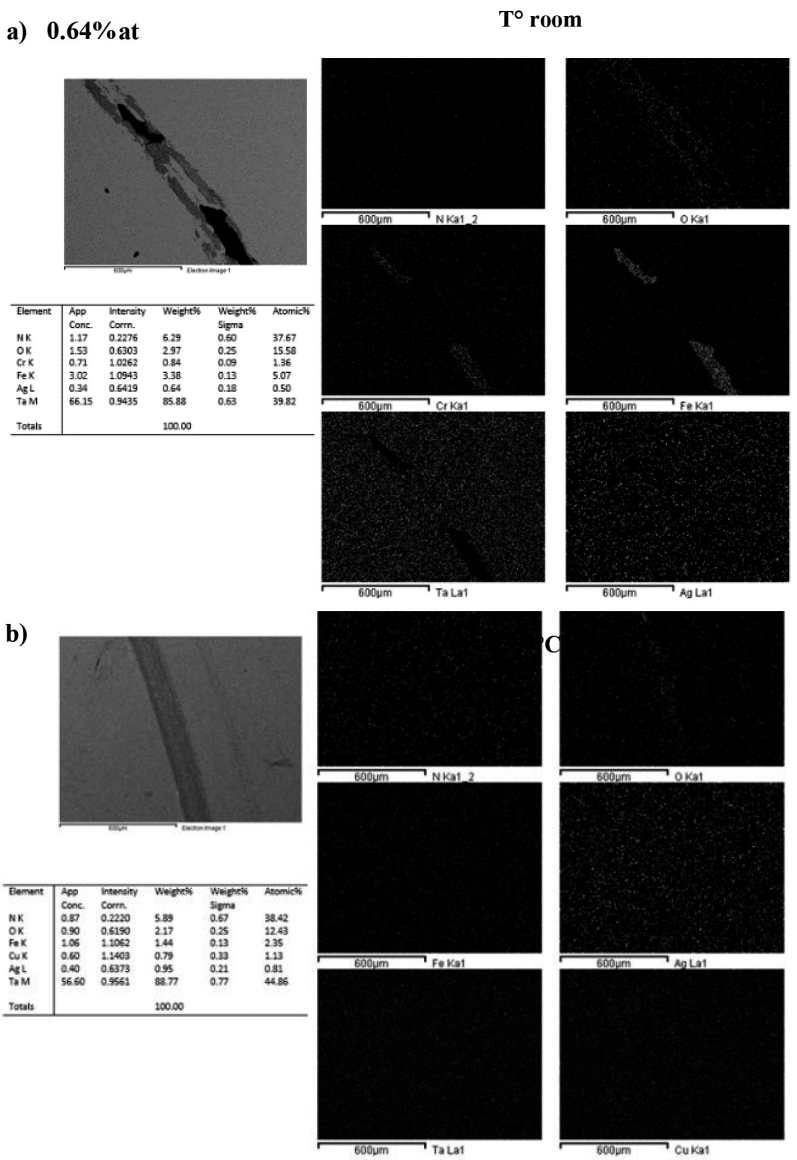

Figure 10. Wear tracks EDX mappings for the coatings a) C1 before heat treatment b) C3 after heat treatment

On the other hand, an elemental homogeneous distribution on the surface of the heat-treated coating was observed (Figure 10b), which indicates that a soft abrasive wear occurred. The cumulative presence of oxygen in the track is probably linked to a tribo-oxidation process.

CONCLUSIONS

TaN(Ag-Cu) coatings were deposited successfully, supplying a constant power of 1500W to Ta-target and 10, 20, 30 and 40W to (Ag-Cu)-target, which presented a hardness between 13.5 GPa and 20.6 GPa, much higher than the heat treated AISI 420 stainless steel of 4.8 GPa, and wear rates six orders of magnitude less than the steel.

Compared to the expensive process of RTA (Rapid Thermal Annealing), the heat treatment of the coated samples in this work was done effectively using a conventional oven operated with a controlled argon-nitrogen atmosphere and cooling the samples with the pressurized air from a fan. The average diameter of the nanoparticles obtained after heat treatment ranged from 15 to 20 nm.

Hardness/wear rate ratio of the coated samples was improved by heat treatment at 250 ºC for 8 minutes due to an appropriated size, form and density of Ag-Cu nanoparticles on coatings surface, demonstrating their effect of solid lubrication efficiently.

Nanocomposites developed in this work, especially C3 coating, have a promising potential for application in cutting and forming tools, as well as in surgical and dental instruments, where an appropriate combination of high hardness and good wear resistance is required.

ACKNOWLEDGEMENT

This work was supported by Departamento Administrativo de Ciencia, Tecnología e Innovación COLCIENCIAS [RC. 0940-2012].

REFERENCES

[1] C. Toughest and M. Machinable. “Type 420M Stainless Steel”. A. Finkl & Sons Co. 2011.

[2] Atlas Speciality Metals. “Stainless Steel Bar 420”, pp. 1-3. April. 2006.

[3] G. Metals. “Stainless steel - 420”. 1991.

[4] J.H. Hsieh, C.C. Tseng, Y.K. Chang, S. Y. Chang and W. Wu. “Antibacterial behavior of TaN-Ag nanocomposite thin films with and without annealing”. Surf. Coatings Technol. Vol. 202 Nº 22-23, pp. 5586-5589. August, 2008.

[5] C.P. Mulligan and D. Gall. “CrN-Ag self-lubricating hard coatings”. Surf. Coatings Technol. Vol. 200 Nº 5-6, pp. 1495-1500. November, 2005.

[6] M. Baraket, D. Mercs, Z.G. Zhang and C. Coddet. “Mechanical and tribological properties of CrN/Ag and CrSiN/Ag nanoscale multilayers”. Surf. Coatings Technol. Vol. 204 Nº 15, pp. 2386-2391. 2010.

[7] A.M. Ć and P. Terek. “Mechanical and tribological properties of nanolayered TiAlN/TiSiN coating”. In 14th International Conference on Tribology - Serbiatrib ‘15, pp. 137-142. 2015.

[8] J. Nohava and P. Dessarzin. “Characterization of tribological behavior and wear mechanisms of novel oxynitride PVD coatings designed for applications at high temperatures”. Tribol. Int. Vol. 81, pp. 231-239. 2015.

[9] A.D. Pogrebnjak, O.M. Ivasishin and V. M. Beresnev. “Arc-Evaporated Nanoscale Multilayer Nitride-Based Coatings for Protection Against Wear, Corrosion, and Oxidation”, pp. 1-28. 2016.

[10] B. Ratner, A. Hoffman, F. Schoen and J. Lemons. “Biomaterials Science: an introduction to materials in medicine”. Estados Unidos: Academic Press. 1996.

[11] T. Riekkinen, J. Molarius, T. Laurila, A. Nurmela, I. Suni, and J. K. Kivilahti. “Reactive sputter deposition and properties of TaxN thin films”. Elseviersevier. Vol. 64, pp. 289-297. 2002.

[12] M. Stavrev, D. Fischer, C. Wenzel, K. Drescher, and N. Mattern. “Crystallographic and morphological characterization of reactively sputtered Ta, TaN and TaNO thin films”. Thin Solid Films. Vol. 307, pp. 79-88. 1997.

[13] Y. Wang, J. Wang, G. Zhang, L. Wang, and P. Yan. “Microstructure and tribology of TiC(Ag)/a-C:H nanocomposite coatings deposited by unbalanced magnetron sputtering”. Surf. Coatings Technol. Vol. 206, pp. 3299-3308. 2012.

[14] D. Babonneau, T. Cabioc, A. Naudon, J.C. Girard and M.F. Denanot. "Silver nanoparticles encapsulated in carbon cages obtained by co-sputtering of the metal and graphite". Vol. 409, pp. 358-371. 1998.

[15] P. Eklund, T. Joelsson, H. Ljungcrantz, O. Wilhelmsson, Z. Czigány, H. Högberg and L. Hultman. "Microstructure and electrical properties of Ti-Si-C-Ag nanocomposite thin films". Surf. Coatings Technol. Vol. 201, pp. 6465-6469. 2007.

[16] H.J. Johnston, G. Hutchison, F.M. Christensen, S. Peters, S. Hankin and V. Stone. "A review of the in vivo and in vitro toxicity of silver and gold particulates: particle attributes and biological mechanisms responsible for the observed toxicity". Crit. Rev. Toxicol. Vol. 40 Nº 4, pp. 328-346. April, 2010.

[17] J.R. Morones-Ramirez, J.A. Winkler, C.S. Spina and J.J. Collins. "Silver Enhances Antibiotic Activity Against Gram-Negative Bacteria". Sci. Transl. Med. Vol. 5, pp. 1-11. 2013.

[18] S. Zhang, D. Sun, Y. Fu and H. Du. "Effect of sputtering target power on microstructure and mechanical properties of nanocomposite nc-TiN y a-SiN x thin films". Vol. 448, pp. 462-467, 2004.

[19] J. Musil and J. Vlcek. "Magnetron sputtering of hard nanocomposite coatings and their properties". Surf. Coatings Technol., pp. 557-566. 2001.

[20] J.R. Lloyd and S. Nakahara. "Voids in thin as deposited gold films prepared by vapor deposition". J. Vac. Sci. Technol. Vol. 14 Nº 1, pp. 655-659. 1977.

[21] I. Petrov, P.B.B. Barna, L. Hultman and J.E.E. Greene. "Microstructural evolution during film growth". J. Vac. Sci. Technol. A Vacuum, Surfaces, Film. Vol. 21 Nº 5, pp. S117. 2003.

[22] P.B. Barna and M. Adamik. "Fundamental structure forming phenomena of polycrystalline films and the structure zone models". Thin Solid Films. Vol. 317, pp. 27-33. 1998.

[23] Z. Li, S. Miyake and Y. Wu. "Effects of Copper Doping on Structure and Properties of TiN Films Prepared by Magnetron Sputtering Assisted by Low Energy Ion Flux Irradiation". Jpn. J. Appl. Phys. Vol. 45 Nº 6A, pp. 5178-5182. 2006.

[24] P. Zeman. "Structure and properties of hard and superhard Zr - Cu - N nanocomposite coatings". Vol. 289, pp. 189-197. 2000.

[25] S. Mardani, H. Norström, U. Smith, J. Olsson and S.-L. Zhang. "Influence of tantalum/tantalum nitride barriers and caps on the high-temperature properties of copper metallization for wide-band gap applications". Microelectron. Eng., Vol. 137, pp. 37-42. 2015.

[26] Y. Wang, J. Wang, G. Zhang, L. Wang and P. Yan. "Microstructure and tribology of TiC(Ag)/a-C:H nanocomposite coatings deposited by unbalanced magnetron sputtering". Surf. Coatings Technol. Vol. 206 Nº 14, pp. 3299-3308. 2012.

[27] C.C. Tseng, J.H. Hsieh, W. Wu, S.Y. Chang and C.L. Chang. "Emergence of Ag particles and their effects on the mechanical properties of TaN-Ag nanocomposite thin films". Surf. Coatings Technol. Vol. 201, pp. 9565-9570. 2007.

[28] S.B. Simonsen, I. Chorkendorff, S. Dahl, M. Skoglundh, J. Sehested and S. Helveg. "Direct observations of oxygen-induced platinum nanoparticle ripening studied by in situ TEM". J. Am. Chem. Soc. Vol. 132 Nº 7, pp. 7968-7975. 2010.

[29] M. José-Yacaman, C. Gutierrez-Wing, M. Miki, D.-Q. Yang, K. N. Piyakis and E. Sacher. "Surface diffusion and coalescence of mobile metal nanoparticles". J. Phys. Chem. B. Vol. 109 Nº 19, pp. 9703-11. May, 2005.

[30] H.B. Liu, M. José-Yacaman, R. Perez, and J.A. Ascencio. "Studies of nanocluster coalescence at high temperature". Appl. Phys. A Mater. Sci. Process. Vol. 77, pp. 63-67. 2003.

[31] A.A. Yanovska, A.S. Stanislavov and L. B. Sukhodub. "Silver-doped hydroxyapatite coatings formed on Ti-6Al-4V substrates and their characterization". Mater. Sci. Eng. C. Vol. 36 Nº 1, pp. 215-220. 2014.

[32] E. Albert and P.A. Albouy. "Antibacterial properties of Ag-TiO2 composite sol-gel coatings". RSC Adv., pp. 59070-59081. 2015.

[33] L. Li, Y. Xu and Z. Zhou. "The Effects of Cu-doped TiO2 Thin Films on Hyperplasia, Inflammation and Bacteria Infection". Appl. Sci. Vol. 5 Nº 4, pp. 1016-1032. 2015.

[34] D.S. Stone, J. Migas, A. Martini, T. Smith, C. Muratore, A.A. Voevodin, and S.M. Aouadi. "Adaptive NbN/Ag coatings for high temperature tribological applications". Surf. Coatings Technol. Vol. 206 Nº 19-20, pp. 4316-4321. 2012.

[35] S.M. Aouadi, D.P. Singh, D.S. Stone, K. Polychronopoulou, F. Nahif, C. Rebholz, C. Muratore, and A.A. Voevodin. "Adaptive VN/Ag nanocomposite coatings with lubricious behavior from 25 to 1000 ºC". Acta Mater. Vol. 58 Nº 16, pp. 5326-5331. 2010.

[36] M. Folkenant, K. Nygren, P. Malinovskis, J. Palisaitis, P. O. Å. Persson, E. Lewin and U. Jansson. "Structure and properties of Cr-C/Ag films deposited by magnetron sputtering". Surf. Coatings Technol. Vol. 281, pp. 184-192. 2015.

[37] K. Holmberg. "A concept for friction mechanisms of coated surfaces". Surf. Coatings Technol. Vol. 56 Nº 1, pp. 1-10. December, 1992.